Identification of the amino acids residues involved in hemagglutinin-neuraminidase of Newcastle disease virus binding to sulfated *Chuanmingshen violaceum* polysaccharides

Xu Song,[1] Lin Liu,[1] Wei Hu,[1] Xiaoxia Liang, Changliang He, Lizi Yin, Gang Ye, Yuanfeng Zou, Lixia Li, Huaqiao Tang, Renyong Jia, and Zhongqiong Yin[2]

Natural Medicine Research Center, College of Veterinary Medicine, Sichuan Agricultural University, Chengdu, 611130 China

ABSTRACT The antiviral mechanism of sulfated polysaccharides is supposed to prevent virus entry, which is mediated by the interactions of anionic charges on sulfated polysaccharides with positively charged domains of viral envelope glycoproteins, leading to shielding of the functional domain involved in virus attachment to cell surface receptors. But, few direct evidences were reported. In the previous study, we found that sulfated *Chuanmingshen violaceum* polysaccharides (**sCVPS**) possessed remarkable inhibitory effect against Newcastle disease virus (**NDV**) through inhibition of NDV attachment to host cells. Whether sCVPS bound to hemagglutinin-neuraminidase (**HN**) leading to inhibition of NDV attachment needs to be further clarified. The present study conducted site-directed mutagenesis of possible positively charged residues of HN, and found that mutants R197G, H199G, R363G, and R523G could significantly decrease the inhibitory effects of sCVPS on receptor binding ability through hemadsorption assay, especially R363G which suggested that binding to R363 is more effective to shield the sialic acid binding sites. Dual mutants (R363G/R197G, R363G/H199G and R363G/R523G) induced more decreased inhibitory effect of sCVPS than single mutants. The immunofluorescence study using FITC-labeled sCVPS found that the fluorescence intensity of mutants R363G and R363G/H199G were significantly decreased. The binding kinetics of sCVPS to HN measured by surface plasmon resonance indicated that sCVPS had a higher binding affinity for wild-type HN than mutants R363G and R363G/H199G. Plaque reduction study was performed using recombinant NDV with mutant HN_{R363G} and $HN_{R363G/H199G}$, which showed significantly decreased inhibitory effects of sCVPS against mutant NDV adsorption to BHK-21 cells. These results suggested that the residues R197, H199, R363, and R523 were the binding sites for sCVPS, especially R363 act as the main interaction site. The present study provided direct evidence for the theory that antiviral mechanism of sulfated polysaccharides attributed to anionic groups binding to the positively charged residues of viral proteins which led to the shielding of receptor binding sites.

Key words: Newcastle disease virus, sulfated *Chuanmingshen violaceum* polysaccharides, hemagglutinin-neuraminidase, interaction sites

2021 Poultry Science 100:101255
https://doi.org/10.1016/j.psj.2021.101255

INTRODUCTION

Newcastle disease virus (**NDV**), a member of the species *Avian avulavirus 1* of the genus *Orthoavulavirus* of the *Paramyxoviridae* family, is a nonsegmented negative-sense single-stranded RNA virus (Maan et al., 2019). NDV can infect over 250 species of avian family, causing significant global economic losses to domestic poultry industry (Diel et al., 2012). NDV isolates are classified into 2 classes (class I and class II) which are further separated into multiple genotypes, especially in class II there are 20 genotypes (I to XXI except XV) and several sub-genotypes (Dimitrov et al., 2019a). Due to rapid evolution and genetic diversity, outbreaks of NDV infections caused by virulent strains repeatedly happen, suggesting current vaccines couldn't provide full protection against emerging strains (Dortmans et al., 2012; Nath et al., 2016; Dimitrov et al., 2019b). Thus, NDV infections show significant difficulties to disease control

Received March 3, 2021.
Accepted May 5, 2021.

[1]These authors contribute equally to this work and should be considered as the first author.

[2]Corresponding author: yinzhongq@163.com

strategies and alternative control measures are urgently needed.

The RNA genome of NDV is approximately 15-kb long and encodes 6 major structural proteins (3′−5′): nucleoprotein (**NP**), phosphoprotein (**P**), matrix protein (M), fusion protein (**F**), hemagglutinin-neuraminidase (**HN**), and large polymerase protein (L) (Shahar et al., 2018). HN, one of the 2 surface glycoproteins, is responsible for the binding of the virion to sialic acid-containing receptors on the host cell surface, which is the first step of NDV infection (Jin et al., 2016). After attachment, HN cooperates with another surface glycoprotein, F, facilitating membrane fusion to allow the entry of viral RNA into host cell (Porotto et al., 2011). In addition, HN possesses neuraminidase (NA) activity to hydrolyze the sialic acid molecules from progeny virions to avoid self-aggregation (Connaris et al., 2002). It exists in the form of a homotetramer containing an N-terminal transmembrane domain followed by an ectodomain that comprised of a stalk region and a large C-terminal globular head domain (Yuan et al., 2012). The stalk region can interact with the homologous F protein, promoting fusogenic activity (Melanson and Iorio, 2006). The major amino acid residues located in the globular head are related to the receptor recognition of sialic acid and NA activities (Crennell et al., 2000; Iorio et al., 2001). The structure of the ectodomain shows that the stalk forms a parallel tetrameric coiled-coil bundle and

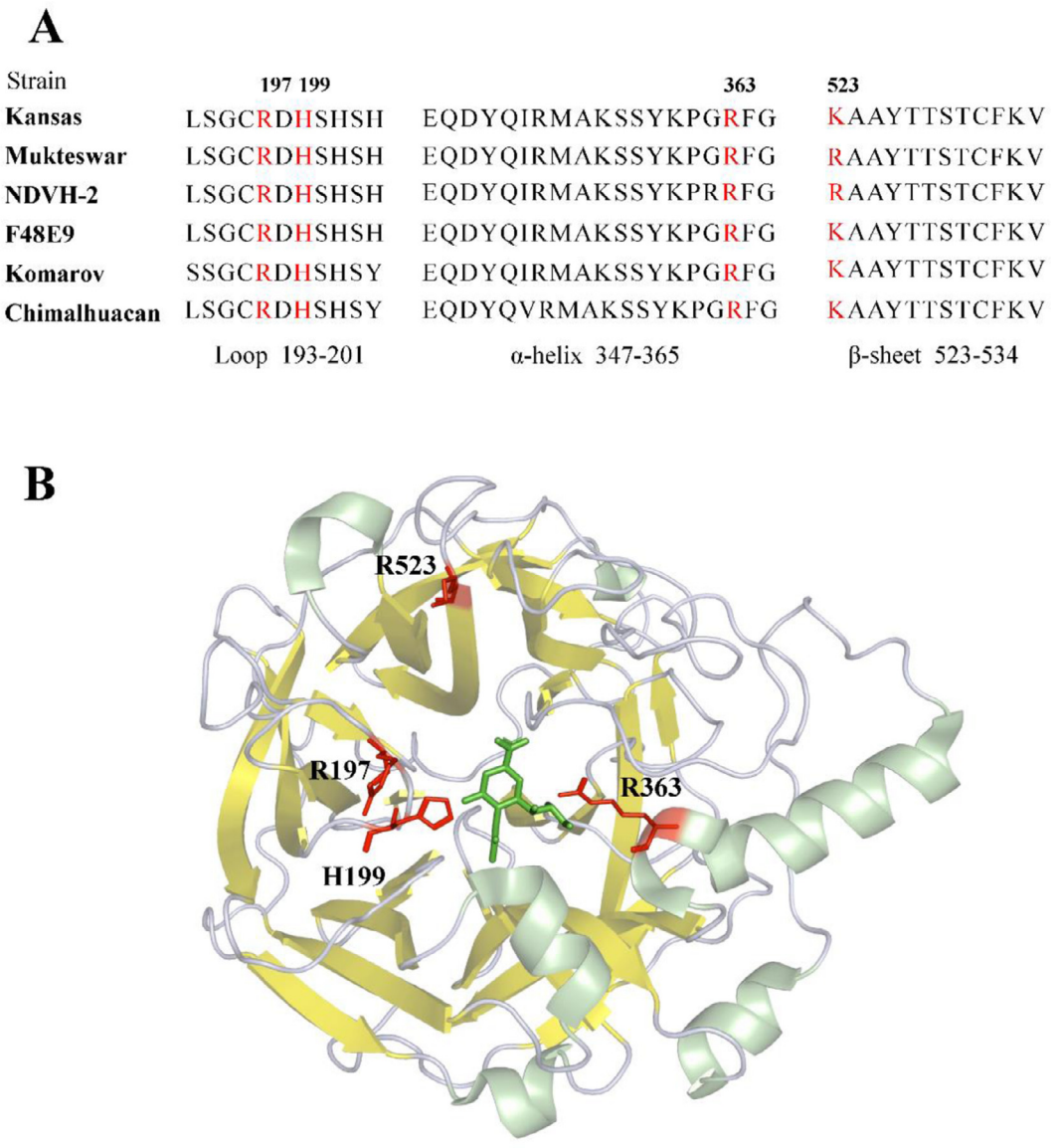

Figure 1. Sequence alignment and location of the desired amino acid residues. (A) sequence alignment of the four amino acid residues in red from six strains of HN based on the structure of Kanas strain (Crennell et al., 2000). (B) the location of the four amino acid residues. The crystal structure (PDB ID: 1e8u) of the globular head domain of the NDV HN monomer was shown as cartoon mode generated by PyMOL 2.5.0. The structure of α-helix, β-sheet and loop were shown in lime, yellow, and grey, respectively. The four residues are shown as stick mode which was colored red. The receptor sialic acid in green is located at the center of the β-propeller fold. Abbreviations: HN, hemagglutinin-neuraminidase; sCVP, sulfated Chuanmingshen violaceum polysaccharides; NDV, Newcastle disease virus.

Table 1. Mutant primer sequences.

Mutant	Forward Primers (5′−3′)	Reverse Primers (5′−3′)
R197G	ATATTGTCTGGCTGC**G**GAGATCACTC	**C**GCAGCCAGACAATATCACATTGTGAG
H199G	TCTGGCTGCAGAGAT**GG**CTCACACTCAC	**CC**ATCTCTGCAGCCAGACAATATCACAT
R363G	TCGTATAAGCCTGGG**C**GGTTTGGTGG	**C**CCCAGGCTTATACGATGACTTAGCC
R523G	AGTTCAAGCAGTACC**G**GGGCAGCATAC	**C**GGTACTGCTTGAACTTACCCGAGTT

The single amino acid mutations, R197G, H199G, R363G and R523G, were achieved by site-directed mutagenesis. The plasmid pcDNA3.1-HN was used as the template. The primers were introduced with changed base pairs corresponding to the mutation site (Framed). For obtaining dual mutations, R363G/R197G, R363G/H199G, and R363G/R523G, the mutant plasmid pcDNA3.1-HN_{R363G} was used as the template and the primers were the same as the corresponding single amino acid mutation.

the globular head forms a six-bladed β-propeller fold (Figure 1) (Yuan et al., 2011).

Sulfated polysaccharides have sulfate groups esterified with the polysaccharide hydroxyl groups. A large number of sulfated polysaccharides, both chemically synthesized and naturally extracted, have been found to possess abroad spectrum of antiviral activity (Wijesekara et al., 2011; Chen and Huang, 2018; Wang et al., 2018). The antiviral mechanism of sulfated polysaccharides attributed to prevention of virus entry, which is mediated by the interactions of anionic charges in sulfated polysaccharides with positively charged domains of viral envelope glycoproteins, leading to shielding of the functional domain involved in virus attachment to cell surface receptors (Damonte et al., 2004; Pujol et al., 2007). Recently, it has been demonstrated that the anti-HIV activity of sulfated polysaccharides attributed to interaction between the negatively charged sulfate groups and positively charged amino acid regions in the HIV gp120 (Battulga et al., 2019). However, little study was conducted to identify which positively charged residues were interacted with sulfated polysaccharides. Previously, we conducted sulfated modification of *Chuanmingshen violaceum* polysaccharides (**sCVPS**), and found that sCVPS possessed remarkable inhibitory effect of NDV both in vitro (Song et al., 2013b) and in vivo (Song et al., 2015). The sCVPS could inhibit NDV attachment to host cells, suggesting that sCVPS competitively inhibited the binding of NDV to sialic acid receptors on the cell surface. Therefore, this study was conducted to elucidate the amino acid residues on HN that responsible for binding to sCVPS.

MATERIALS AND METHODS

sCVPS

sCVPS are obtained by sulfated modification of *Chuanmingshen violaceum* polysaccharides with the chlorosulfonic acid-pyridine method. The sulfur content (S %) of sCVPS used in this study was 11.71% and the degree of sulfation was 0.95. The average molecular weight of sCVPS was 2.54×10^5 Da. The sCVPS is composed of D-carubinose and D-glucose with a ratio of 1:16.2 (Song et al., 2013a).

Fluorescein isothiocyanate (**FITC**) -labeled sCVPS (sCVPS-FITC) were prepared using the method described by Tanaka et al., 2004. Briefly, sCVPS (300 mg) was dissolved in dimethyl sulfoxide (10 mL) and allowed to react with FITC (400 mg) and dibutylin dilaurate (20 mg) for 2 h at 95°C with intermittent mixing. After precipitations in ethanol for three times, the FITC-labeled sCVPS was purified by size-exclusion chromatography on a Sephadex G-25 column and then freeze-dried to give sCVPS-FITC.

Cells, Vectors, and Recombinant Plasmids

The human kidney epithelial 293T and BHK-21 cells were grown in Dulbecco's modified Eagle's medium (DMEM) supplemented with 10% (v/v) fetal calf serum (Hyclone), 100 U/mL penicillin, and 100 μg/mL streptomycin at 37°C and 5% CO_2. The HN gene of NDV (Mukteswar strain; Gene bank: JF950509.1) was synthesized by the GENEWIZ Biotechnology Co., Ltd (Suzhou, China) and subcloned into the transient mammalian expression vector pcDNA3.1 using HindIII and BamHI restriction enzyme sites (Invitrogen). For protein expression, a cDNA fragment encoding the globular head domain of wild-type or mutant HN (residues 147−571), was cloned into a modified pcDNA3.1 +hygromycin vector (Invitrogen) containing secretion signal and removable C-terminal Fc tag by thrombin cleavage site.

Site-Directed Mutagenesis

Mutants of NDV HN, including R197G, H199G, R363G and R523G, were achieved using the Fast Site-Directed Mutagenesis kit (TIANGEN, Beijing, China). The primers used to introduce single amino acid mutations in the HN gene were designed according to manufacturer's instruction (Table 1). After amplification by PCR using the pcDNA3.1-HN as the template, the product was digested by the *Dpn* I restriction enzyme for removal of the template plasmid. The digested product was transformed into FDM competent cells, and plasmid DNA from colonies was fully sequenced to confirm the presence of desired mutation. Dual amino acid mutations, including R363G/R197G, R363G/H199G, and R363G/R523G, were also accomplished using the mutant plasmid pcDNA3.1-HN_{R363G} as the template.

Immunofluorescence Assay

293T cells grown to 80% confluency in 6-well plates were transfected with 2 μg of plasmid (wild-type or

mutant HN) diluted in 200 μL jetPRIME buffer (Polyplus-transfection SA) for 4 h at 37°C. The transfection medium was replaced with grown medium and cells were incubated for 24 h. The cells were fixed with 4% paraformaldehyde for 15 min, blocked with 2% bovine serum albumin for 1 h and incubated with HN monoclonal antibody at 4°C overnight. After washing, the cells were incubated by FITC-labeled goat anti-mouse IgG (Beyotime, China) for 30 min, and subsequently incubated with DAPI for 5 min. The fluorescence was observed by an inverted fluorescence microscope (Olympus, Japan). For detecting the binding of sCVPS to HN, the sCVPS-FITC was incubated with transfected cells instead of HN antibody at 4°C for 30 min, and the secondary antibody is no longer used for observation.

Hemadsorption Assay

The ability of wild-type HN and mutants to adsorb chicken erythrocytes was evaluated to determine the receptor binding activity as described by Connaris et al. (2002). The 293T monolayers about 80% confluency grown in 24-well plates were transfected with HN wild-type or mutant plasmids by the jetPRIME buffer following the manufacturer's instruction. After incubation for 24 h, transfected 293T cells were washed with PBS buffer prior to addition of 2% (v/v) chicken erythrocyte suspension in the absence or presence of 200 μg/mL sCVPS. The plates were placed at 4°C for 30 min. The cells were washed three times gently with cold PBS for removal of unadsorbed erythrocytes, and subsequently treated with 50 mM NH_4Cl at 4°C to lyse bound erythrocytes. The absorbance of lysate was read at 405 nm with a UV spectrophotometer (Shimadzu, Japan). The inhibitory effects of sCVPS on receptor binding ability of HN were determined according to the formula: inhibitory rate = (OD_{405nm} values of untreated cells - OD_{405nm} values of sCVPS-treated cells) ÷ OD_{405nm} values of untreated cells.

Surface Plasmon Resonance Assay

A 293T stable cell line expressing the globular head domain of wild-type or mutant HN (R363G and R363G/H199G) was generated. The cell medium containing the secreted recombinant proteins was collected and loaded onto a Protein A-Sepharose affinity column (GE Biosciences), followed by elution with low-pH buffer containing 150 mM NaCl and 100 mM glycine (pH 3.0). The Fc tag was cleaved by thrombin proteolysis and removed by Protein A-Sepharose. The recombinant HN proteins were further purified by gel filtration chromatography on a Superdex G200 size-exclusion column (GE Biosciences).

The surface plasmon resonance (**SPR**) assays were performed on an OpenSPR (Nicoya Lifesciences, Waterloo, Canada) to determine the kinetics of sCVPS-HN interaction. The purified wild-type or mutant HN proteins were diluted in the immobilization buffer to a volume of 200 μL at a concentration around 1 mg/mL, followed by immobilization on a COOH sensor chip according to manufacturer's instruction, respectively. The sCVPS (100 μM) in PBS running buffer was passed over the immobilized wild-type or mutant HN proteins, respectively. The interaction of sCVPS with the fixed HN proteins was detected by OpenSPR at RT. The binding time was 240 s, and the disassociation time was 300 s, the flowrate was 20 μL/min. The data was analyzed and fitted with 1:1 binding model with TraceDrawer software (Ridgeview Instruments AB, Sweden) to give the association rate (Ka), the dissociation rate (Kd), and the dissociation constant (assuming the relationship KD = Kd / Ka) (Lu et al., 2019).

Recovery of Recombinant NDV

The recombinant NDV was rescued according to the methods described by Römer-Oberdörfer et al., 1999. The cDNA of NDV (Mukteswar strain; Gene bank: JF950509.1) with mutant sites (HN_{R363G} or $HN_{R363G/H199G}$) was cloned to pVAX plasmid (Invitrogen) which contained T7 promoter sequence at the 5' end and ribozyme sequence of Hepatitis delta virus and T7 RNA polymerase terminator sequence at the 3' end (pNDV-HNR363G and pNDV-HNR363G/H199G; Kangruiyuan Biotechnology Co., Ltd, Chengdu, China). The open reading frames of NP (nt 122-1591), P (nt 1887-3071) and L (nt 8381-14995) were cloned into pVAX plasmids, respectively. The BSR-T7/5 cells with 80% confluence in 60-mm diameter dishes, stably expressing the phage T7 RNA polymerase, were transfected with a total amount of 10 μg DNA (5 μg pNDV-HNR363G or pNDV-HNR363G/H199G, 2 μg pVAX-NP, 2 μg pVAX-P and 1 μg pVAX-L) diluted in 500μL jetPRIME buffer (Polyplus-transfection SA) for 4 h at 37°C. The transfection medium was replaced with grown medium and cells were incubated for 72 h. The transfected cells were harvested by thrice freeze-thaw cycles. After centrifugation at 12,000 *g* for 15 min, 100 μL supernatant was inoculated into the allantoic cavity of 10-day-old embryonated SPF chicken eggs (Sais Poultry Co., LTD, Jinan, China) to amplify the recovered recombinant virus. After inoculation for 3 d, the allantoic fluid was harvested and tested for hemagglutinating activity. The allantoic fluid with positive hemagglutinating activity were used for reverse transcription PCR assay, followed by sequencing for confirming the HN mutant sites. Then, the confirmed mutant NDV strains, rNDV-HNR363G and rNDV-HNR363G/H199G, were propagated in 10-day-old embryonated SPF chicken eggs.

For evaluating growth characteristics of recombinant NDV, BHK-21 cells grown in 6 well plates were infected with wild-type NDV, rNDV-HNR363G and rNDV-HNR363G/H199G at a MOI of 0.1. Total RNA was extracted from cells using RNA Extraction Kit

(No.9767; Takara) according to the manufacturer's instructions at 4, 8, 12, 16, and 20 h postinfection. The genome copies were quantified by real-time RT-PCR method as described by Song et al., 2013b.

For further confirming the interaction sites of sCVPS with HN, plaque reduction assay was performed (Song et al., 2013b). Briefly, BHK-21 cells grown in 6 well plates were infected with NDV, rNDV-HNR363G and rNDV-HNR363G/H199G at a PFU of 50 in the presence or absence of sCVPS (200 μg/ mL). After 1 h incubation at 37°C, monolayers were washed three times with cold PBS to remove uninfected viruses and the medium containing 1% methylcellulose was added. After 60 h incubation, the cells were stained with 0.1% crystal violet in 20% methanol. Plaques were counted and the inhibitory rate was calculated according to the formula: inhibitory rate = (number of plaques in infected-untreated group - number of plaques in infected-treated group) ÷ number of plaques in infected-untreated group.

Statistical Analysis

The data are presented as the mean ± standard deviation. The statistical significance was compared between the wide-type group and mutant groups by one-way analysis of variance (ANOVA) followed by the Student −Newman−Keuls test using the IBM SPSS Statistics, Version 24 program (IBM Corporation. Somers, NY). The differences between groups would be considered significant when values of $P < 0.05$. Graphs were plotted and analyzed using GraphPad Prism software, version 8.0 (GraphPad Software, La Jolla, CA).

RESULTS

sCVPS Inhibited Receptor Binding Ability of Wild-Type HN and Mutants

The 293T cells were transfected with wild-type or mutant HN plasmids, and the expression of HN protein was detected by indirect immunofluorescence. The results (Figure 2) showed that the fluorescence except plasmid control group could be observed, suggesting that wild-type and mutant HN could express in 293T cells. Then, the receptor binding activities of wild-type HN and mutants were determined through hemadsorption assay in order to confirm whether mutation of these amino acids would affect the receptor binding ability of HN. The absorbances of the lysates from bound erythrocytes showed that wild-type and mutant HN did not show any significant differences ($P > 0.05$) in receptor binding ability (Figure 3A). The HN mutants R197G and H199G induced slight decrease in hemadsorption ability. The receptor binding ability of mutants R197G and H199G was reduced to 91.3% and 94.10% of wild-type HN (Figure 3B). The HN mutants R363G and R523G showed equal hemadsorption ability to wild-type HN.

The HN mutants did not significantly affect the receptor binding ability, thus they could be used to test whether sCVPS could bind to these amino acid residues leading to shield the binding sites of sialic acid receptor.

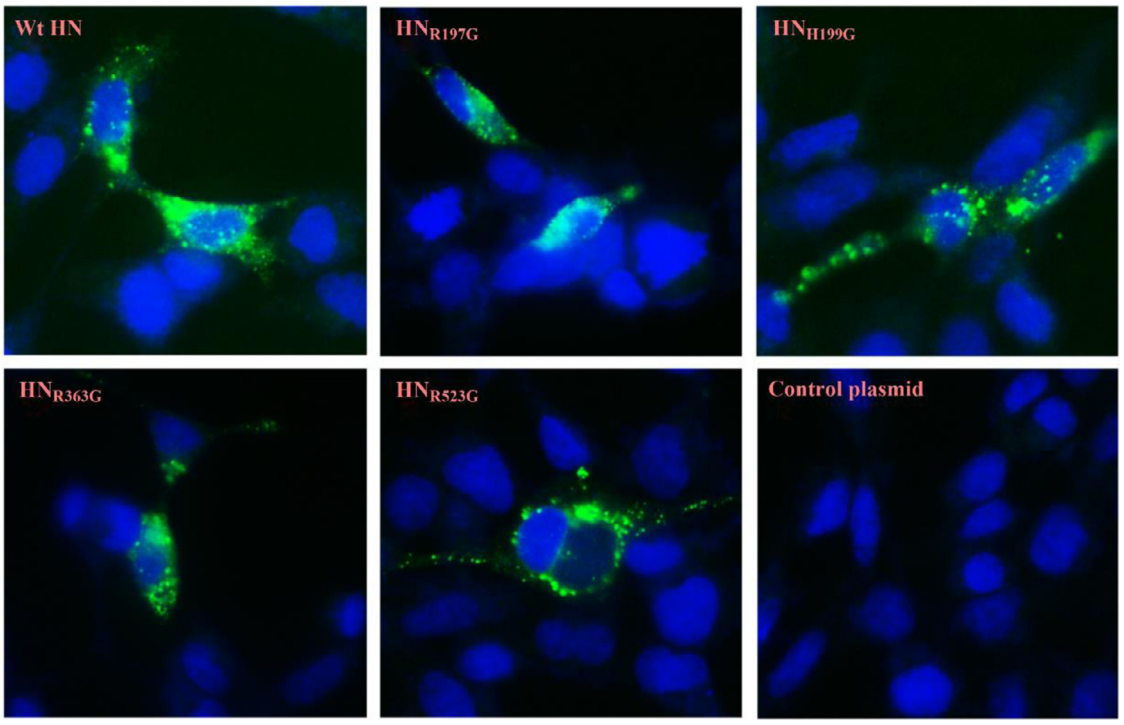

Figure 2. Expressions of wild-type and mutant HN proteins by indirect immunofluorescence. 293T cells were transfected with 2 μg of plasmid (wild-type or mutant HN). After incubation for 24 h, the cells were fixed with 4% paraformaldehyde and blocked with 2% bovine serum albumin, followed by incubation with HN monoclonal antibody at 4°C overnight. After washing, the cells were incubated by FITC-labeled goat anti-mouse IgG, and subsequently incubated with DAPI for 5 min. The fluorescence was observed by an inverted fluorescence microscope.

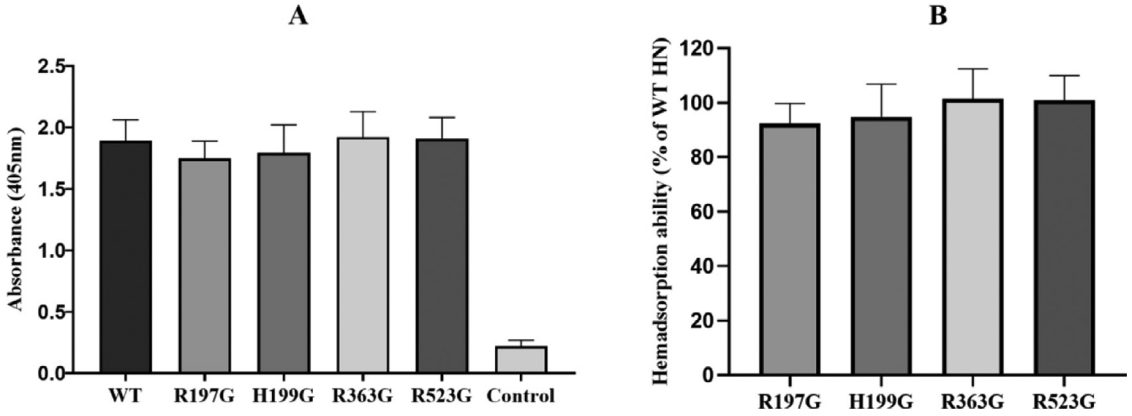

Figure 3. The receptor binding ability of wild-type and mutants HN. (A) the absorbances of the lysates of bound erythrocytes. The 293T cells were transfected with HN wild-type or mutant plasmids. After incubation for 24 h, 2% (v/v) chicken erythrocyte suspension was added followed by incubation at 4°C for 30 min. The cells we re washed gently with cold PBS for removal of unadsorbed erythrocytes, and bound erythrocytes were lysed. The absorbance of lysate was read at 405 nm. (B) hemadsorption ability of mutants HN, and the values were expressed as percentages of that of wild-type HN. $n = 5$. Abbreviations: HN, hemagglutinin-neuraminidase; WT, wild-type HN; Control, pcDNA3.1 plasmid.

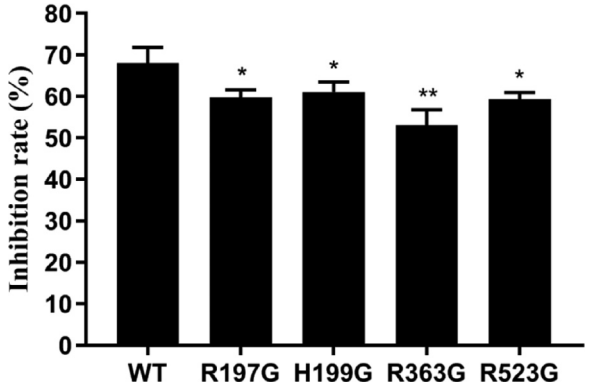

Figure 4. Inhibitory rate of sCVPS against the receptor binding activity of wild-type and mutants. The 293T cells were transfected with HN wild-type or mutants plasmids. After incubation for 24 h, 2% (v/v) chicken erythrocyte suspension was added followed by incubation at 4°C for 30 min in the presence or absence of sCVPS. The cells were washed gently with cold PBS for removal of unadsorbed erythrocytes, and bound erythrocytes were lysed. The absorbance of lysate was read at 405 nm. Inhibitory rate = (OD405 nm values of untreated cells - OD405 nm values of sCVPS-treated cells) ÷ OD405 nm values of untreated cells. $n = 5$; * represents $P < 0.05$ vs. wt HN; ** represents $P < 0.01$ vs. wt HN.Abbreviations: HN, hemagglutinin-neuraminidase; sCVP, sulfated Chuanmingshen violaceum polysaccharides.

The results (Figure 4) showed that sCVPS could inhibit the hemadsorption ability of wild-type HN by 68.06%. The inhibitory effects of sCVPS against the mutants R197G, H199G, R363G, and R523G significantly decreased, and the inhibition rates were 59.80%, 61.05%, 53.08%, and 59.38%, respectively. These results suggested that the mutants decreased the binding of sCVPS with HN.

The mutant R363G had the lowest inhibition rate, thus it was used as the template to construct dual mutants for further confirmation of the binding sites. The hemadsorption ability (Figure 5A) of the mutants R363G/R197G, R363G/H199G and R363G/R523G were 90.60%, 102.82%, and 98.11% of wt HN, respectively, and no significant differences were observed. sCVPS could inhibit the hemadsorption ability of wild-type HN by 69.91%, and the inhibition rates of R363G/R197G, R363G/R523G, R363G/H199G were decreased to 52.88%, 52.90% and 42.68%, respectively (Figure 5B). These results suggested that the dual mutants had lower binding ability to sCVPS when compared with wt HN and single mutants.

Immunofluorescence Study Revealed Decreased Binding of sCVPS to Mutant HN

The receptor binding ability of wt HN and mutants were decreased by sCVPS through hemadsorption assay. In this assay, FITC-labeled sCVPS were used to detect the binding to wt HN and mutants. As shown in Figure 6, fluorescence on the cell surface was observed; compared with wt HN, the fluorescence intensity of mutants R363G and R363G/H199G were significantly decreased, suggesting that the amount of sCVPS bound to the mutants R363G and R363G/H199G were significantly decreased. These results indicated that mutation of R363 and H199 decreased the binding ability of sCVPS to HN.

The Kinetics of sCVPS-HN Interaction by SPR

The mutants R363G and R363G/H199G showed the highest decrease in the binding ability to sCVPS. The interactions of sCVPS with wt HN and mutants were further corroborated using SPR (Figure 7). The equilibrium dissociation constants (Kd) were 1.60×10^{-5} M (wt), 1.33×10^{-4} M (R363G) and 4.19×10^{-4} M (R363G/H199G), respectively. Thus, sCVPS had a higher binding affinity for wt HN than mutants R363G and R363G/H199G. This demonstrated that mutation of arginine at position 363 and histidine at position 199 to glycine decreased sCVPS binding to HN.

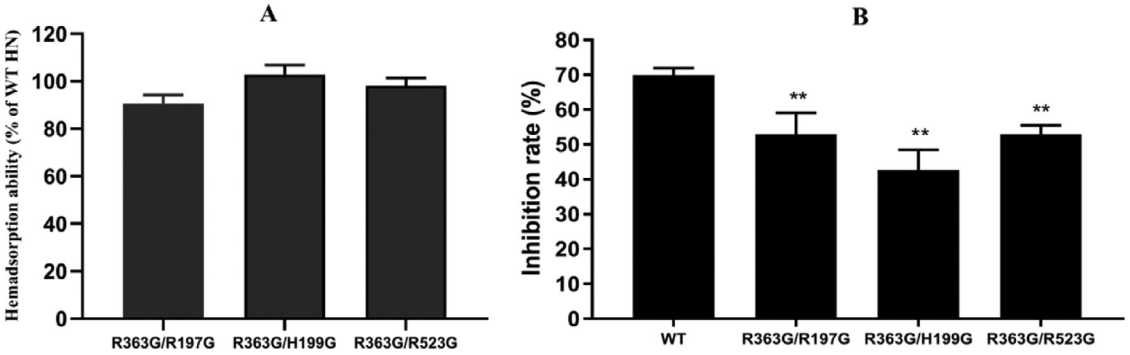

Figure 5. Hemadsorption ability of the dual mutants (A) and Inhibitory rate of sCVPS against the receptor binding activity of the wild-type and dual mutants (B). The 293T cells were transfected with HN wild-type or mutant plasmids. After incubation for 24 h, 2% (v/v) chicken erythrocyte suspension was added followed by incubation at 4°C for 30 min in the presence or absence of sCVPS. The cells were washed gently with cold PBS for removal of unabsorbed erythrocytes, and bound erythrocytes were lysed. The absorbance of lysate was read at 405 nm. Inhibitory rate = (OD_{405nm} values of untreated cells - OD_{405nm} values of sCVPS-treated cells) ÷ OD_{405nm} values of untreated cells. $n = 5$. ** represents $P <$ 0.01 vs. wt HN. Abbreviations: HN, hemagglutinin-neuraminidase; sCVP, sulfated Chuanmingshen violaceum polysaccharides.

Decreased Inhibitory Effects of sCVPS Against Mutant NDV Adsorption

The growth characteristics of recombinant NDV (rNDV-HNR363G and rNDV-HNR363G/H199G) was compared to wt NDV in BHK-21 cells. Both wild-type and recombinant viruses propagated efficiently in cells and showed similar growth characteristics (Figure 8A). These results suggested that wild-type and recombinant NDV had identical biological properties.

To study whether mutant NDV could induce decreased binding ability to sCVPS, the inhibitory effects of sCVPS against NDV adsorption were evaluated by plaque reduction assay. The results (Figure 8B) showed that the inhibitory rate of sCVPS (200 μg/mL) against wild-type NDV adsorption was 75.06%. In contrast, the inhibitory effects against mutant NDV was significantly reduced, and the inhibitory rate was decreased to 50.36% against rNDV-HNR363G/H199G. These results demonstrated that R363 and H199 were the interaction sites of sCVPS with HN.

DISCUSSION

ND ranked fourth in the most important poultry diseases, behind highly pathogenic avian influenza, avian infectious bronchitis, and low pathogenic influenza (Kapczynski et al., 2013). Despite there were many ND vaccines available worldwide, such as live, inactivated and vectored vaccines, repeated outbreaks of ND suggested current vaccination practices alone cannot

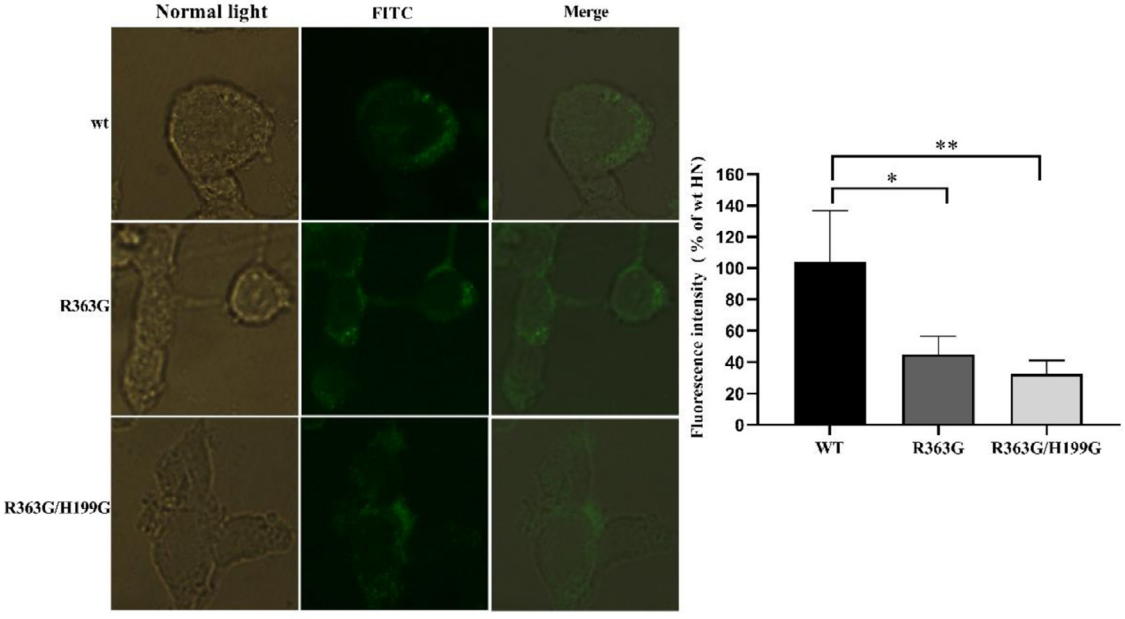

Figure 6. The binding of sCVPS to wild-type and mutant HN by immunofluorescence assay. 293T cells were transfected with 2 μg of plasmid (pcDNA3.1 vector containing HN wild-type or mutant cDNA). After incubation for 24 h, the cells were fixed and blocked, followed by incubation with sCVPS-FITC at 4°C for 30 min. After gently washing, the cells were directly observed by a fluorescence inverted microscope. The images were taken and the fluorescence intensity of fluorescein isothiocyanate were analyzed by the Image J software (Version 1.52, NIH, USA). The data was presented as percentage (%) of wt HN. $n = 5$. * represents $P < 0.05$ vs. wt HN; ** represents $P < 0.01$ vs. wt HN. Abbreviations: HN, hemagglutinin-neuraminidase; sCVP, sulfated Chuanmingshen violaceum polysaccharides.

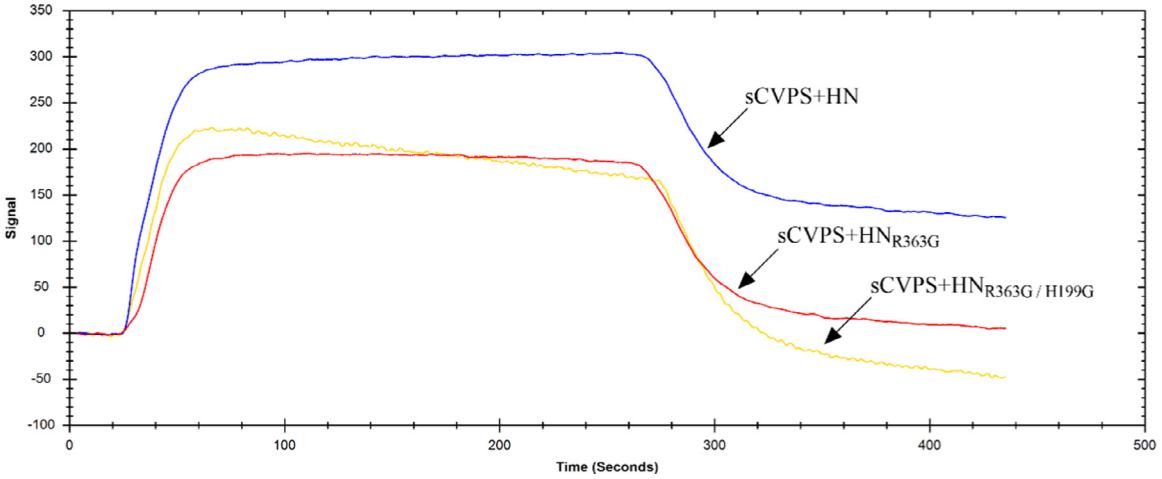

Figure 7. The SPR binding kinetic curves of sCVPS binding to wild-type HN and mutants R363G and R363G/H199G. The wild-type HN and mutant proteins were respectively coupled to COOH sensor chips, and sCVPS was applied at 100 μM. Abbreviations: HN, hemagglutinin-neuraminidase; sCVP, sulfated Chuanmingshen violaceum polysaccharides; SPR, surface plasmon resonance.

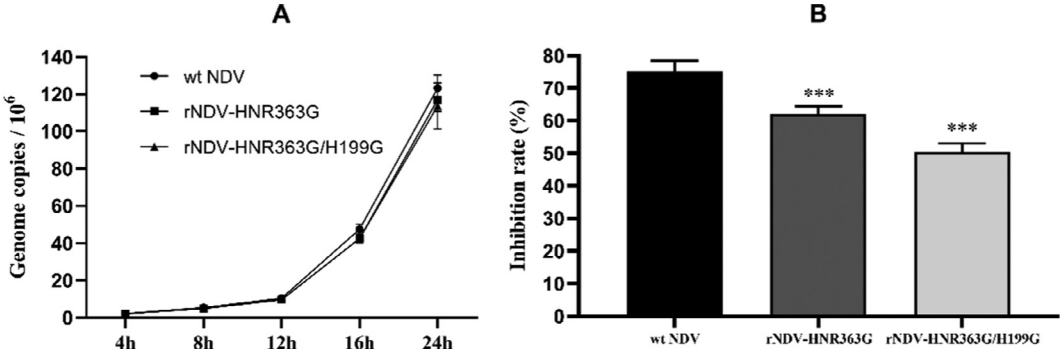

Figure 8. Inhibitory effects of sCVPS against recombinant NDV adsorption. (A) The growth characteristics of recombinant NDV were evaluated by real-time RT-PCR method at 4, 8, 12, 16, and 20 h postinfection. (B) The inhibitory effects of sCVPS against recombinant NDV adsorption was evaluated by plaque reduction assay. BHK-21 cells were infected with NDV at a PFU of 50 in the presence or absence of sCVPS (200 μg/ mL). After 1 h incubation, monolayers were washed and the medium containing 1% methylcellulose was added. After 60 h incubation, the cells were stained with 0.1% crystal violet in 20% methanol. Plaques were counted and the inhibitory rate was calculated according to the formula: inhibitory rate = (number of plaques in infected-untreated group - number of plaques in infected-treated group) ÷ number of plaques in infected-untreated group. $n = 5$. *** represents $P < 0.001$ vs. wt NDV. Abbreviations: sCVP, sulfated Chuanmingshen violaceum polysaccharides; NDV, Newcastle disease virus.

control the disease (Dimitrov et al., 2017). NDV can infect over 236 avian species, but ND vaccination was only applied in the poultry sector, which increased the difficulty to control the disease (Absalón et al., 2019). Thus, searching for complementary control measures are beneficial to poultry industry. Previously, we found that sCVPS could inhibit NDV infection through blocking viral attachment, but the interaction sites with HN were still unknown (Song et al., 2013b, 2015). In this study, the amino acid residues R197, H199, R363, and R523 were demonstrated to be the binding sites for sCVPS, especially R363 act as the main interaction site. These results provide a basis for drug design with these sites.

There were 2 receptor-binding sites located in the globular head domain of HN protein, the site I is a bifunctional site that can mediate sialic-acid-receptor binding and neuraminidase activity and the site Ⅱ is associated with receptor binding which can trigger F activation during fusion process (Zaitsev et al., 2004; Mahon et al., 2011; Porotto et al., 2012). Thus, the site I located at the central of the six-bladed -sheet propeller structure is the main sialic acid binding site for NDV attachment to the host cell (Crennell et al., 2000). The residues R174, I175, E258, Y299, Y317, E401, R416, R498, Y526, and E547 play an important role in receptor binding, and residues E401, R416, and Y526 appear to be key sites for interaction with sialic acid (Connaris et al., 2002). According to the theory that sulfated polysaccharides could bind to positively charged residues leading to shielding of interaction sites of virus with receptors, the positively charged residues of HN including R197, H199, R363, and R523 around the binding sites were selected for testing the hypothesis. There were no reports about the interaction of these residues with receptor binding. This study showed that the hemadsorption abilities of the mutants were not significantly affected (Figure 3), suggesting that mutations of these residues will not affect the structure of HN and these

residues were not involved in receptor binding, which were consisted with previous findings.

The residues R197 and H199 are located at the loop that connected the 2^{th} strand (residues 185−192) with the 3^{th} strand in the 1^{th} β-sheet (residues 202−213) in the globular head of HN; residue R363 is located at the 4^{th} helix (residues 347−363); residue R523 is located at the 1^{th} strand in the 6^{th} β-sheet (residues 523−534) (Zaitsev et al., 2004; Connaris et al., 2002). These 4 positively charged residues are all located on the top of the active site (Figure 1), so when negatively charged polysaccharides bound to these sites could induce shielding of the receptor binding sites. That was demonstrated in this study that mutation of these residues decreased the inhibitory effects of sCVPS (Figure 4). Mutation of residue R363 decreased the most potency of sCVPS in the four residues, suggesting that binding to R363 is more effective to shield the sialic acid binding sites. Further dual mutation based on mutant of residue R363 showed when residues R363 and H199 were all mutated, the anti-NDV activity of sCVPS decreased most in the test single and dual mutants (Figures 4 and 5). The reason should be attribute to the spatial location of R363 and H199 that the two residues are toward the binding pocket of sialic acid, binding to the two residues could be more effective to block receptor binding than R197 and R523 (Figure. 1). For direct observation of sCVPS binding to HN, sCVPS was labeled with fluorescein isothiocyanate, and the binding amount of sCVPS was reflected by fluorescence intensity. This assay (Figure 6) showed consistent results with hemadsorption study that mutation of R363 and H199 decreased the binding ability of HN to sCVPS. There was no live virus involved in the above tests. Whether these interaction sites were correct should be further evaluated in recombinant virus with the sites mutated. The rescued virus with R363G and R363G/H199G mutation of HN revealed a significant reduction of antiviral activity of sCVPS against NDV attachment (Figure 8). The recombinant NDV study demonstrated these residues were the binding sites of sCVPS with HN. The residues R197, H199 and R363 are conserved, while R523 is a nonconservative residue in HN. In most NDV strains, the residue 523 is lysine which is also positively charged residue. Thus the results obtained in this study could also be applied in other strains.

Surface plasmon resonance is a technique that provides real-time monitoring of binding kinetics to characterize the interactions between proteins and proteins / molecules (Vachali et al., 2012; Watrelot et al., 2016). Currently, some studies were conducted to evaluate the interaction of polysaccharides with proteins through SPR (Thompson and Dalgleish, 2010; Gao et al., 2013; Wang et al., 2019). For sulfated polysaccharides, the binding affinity may be associated with sulfated degree (Battulga et al., 2019). The polysaccharides from the ink of cuttlefish *Sepiella maindroni* de Rochebruns showed a reduced binding affinity toward EGFR, when the sulfated degree decreased from 34.7% to 8.2% (Jiang et al., 2018). The structure of polysaccharides varied a lot, which also plays an important role in binding affinity. The KD value was 1.26 μM for pumpkin pectic polysaccharide to Galectin-3, which showed higher binding affinity than that of potato galactan (KD value of 2.59 μM) (Zhao et al., 2017). In the present study, the binding affinity of sCVPS to HN decreased along with the mutation of residues R363 and R363/H199 (Figure 7), suggesting the R363 and H199 involved in interaction with sCVPS which is consistent with the results obtained from hemadsorption assay.

In conclusion, the present study provides direct evidence for the antiviral mechanism of sulfated polysaccharides which binds to the positively charged residues leading to the shielding of receptor binding sites. The residues R197, H199, R363 and R523 of HN interact strongly with sCVPS, especially residue R363 acted as the main site. This study suggests that the anti-NDV activity of sCVPS attributes to electrostatic interaction between the negatively charged sCVPS and positively charged residues of HN.

ACKNOWLEDGMENTS

This work was supported by the National Natural Science Foundation of China (Grant no. 31602110) and the Program Sichuan Veterinary Medicine and Drug Innovation Group of China Agricultural Research System (SCCXTD-2020-18).

Author Contributions: X. S. and Z. Y. designed the study and writing the paper; W. H., L. L., and L. X. performed the experiments; Z. Y., H. T., G. Y., and R. J. analyzed the results; Z. Y. and C. H. reviewed and edited the paper. All authors have read and approved the final manuscript.

DISCLOSURES

The authors report no declarations of interest

REFERENCES

Absalón, A. E., D. V. Cortés-Espinosa, E. Lucio, P. J. Miller, and C. L. Afonso. 2019. Epidemiology, control, and prevention of Newcastle disease in endemic regions: Latin America. Trop Anim Health Prod. 51:1033–1048.

Battulga, T., O. Tumurbaatar, O. Ganzorig, T. Ishimura, T. Kanamoto, H. Nakashima, K. Miyazaki, and T. Yoshida. 2019. Analysis of interaction between sulfated polysaccharides and HIV oligopeptides by surface plasmon resonance. Int. J. Biol. Macromol. 125:909–914.

Chen, L., and G. Huang. 2018. The antiviral activity of polysaccharides and their derivatives. Int. J. Biol. Macromol. 115:77–82.

Crennell, S., T. Takimoto, A. Portner, and G. Taylor. 2000. Crystal structure of the multifunctional paramyxovirus hemagglutinin-neuraminidase. Nat. Struct. Biol. 7:1068–1074.

Connaris, H., T. Takimoto, R. Russell, S. Crennell, I. Moustafa, A. Portner, and G. Taylor. 2002. Probing the sialic acid binding site of the hemagglutinin-neuraminidase of newcastle disease virus: identification of key amino acids involved in cell binding, catalysis, and fusion. J. Virol. 76:1816–1824.

Damonte, E. B., M. C. Matulewicz, and A. S. Cerezo. 2004. Sulfated seaweed polysaccharides as antiviral agents. Curr. Med. Chem. 18:2399–2419.

Dimitrov, K. M., C. L. Afonso, Q. Yu, and P. J. Miller. 2017. Newcastle disease vaccines-A solved problem or a continuous challenge? Vet. Microbiol. 206:126–136.

Dimitrov, K. M., C. Abolnik, C. L. Afonso, E. Albina, J. Bahl, M. Berg, F. X. Briand, I. H. Brown, K. S. Choi, I. Chvala, D. G. Diel, P. A. Durr, H. L. Ferreira, A. Fusaro, P. Gil, G. V. Goujgoulova, C. Grund, J. T. Hicks, T. M. Joannis, M. K. Torchetti, S. Kolosov, B. Lambrecht, N. S. Lewis, H. Liu, H. Liu, S. McCullough, P. J. Miller, I. Monne, C. P. Muller, M. Munir, D. Reischak, M. Sabra, S. K. Samal, R. Servan de Almeida, I. Shittu, C. J. Snoeck, D. L. Suarez, S. Van Borm, Z. Wang, and F. Y. K. Wong. 2019a. Updated unified phylogenetic classification system and revised nomenclature for Newcastle disease virus. Infect. Genet. Evol 74:103917.

Dimitrov, K. M., H. L. Ferreira, M. J. Pantin-Jackwood, T. L. Taylor, I. V. Goraichuk, B. M. Crossley, M. L. Killian, N. H. Bergeson, M. K. Torchetti, C. L. Afonso, and D. L. Suarez. 2019b. Pathogenicity and transmission of virulent Newcastle disease virus from the 2018−2019 California outbreak and related viruses in young and adult chickens. Virology 531:203–218.

Diel, D. G., P. J. Miller, P. C. Wolf, R. M. Mickley, A. R. Musante, D. C. Emanueli, K. J. Shively, K. Pedersen, and C. L. Afonso. 2012. Characterization of Newcastle disease viruses isolated from cormorant and gull species in the United States in 2010. Avian Dis. 56:128–133.

Dortmans, J. C., B. P. Peeters, and G. Koch. 2012. Newcastle disease virus outbreaks: vaccine mismatch or inadequate application? Vet. Microbiol. 160:17–22.

Gao, X., Y. Zhi, L. Sun, X. Peng, T. Zhang, H. Xue, G. Tai, and Y. Zhou. 2013. The inhibitory effects of a rhamnogalacturonan I (RG-I) domain from ginseng pectin on galectin-3 and its structure-activity relationship. J. Biol. Chem. 288:33953–33965.

Iorio, R. M., G. M. Field, J. M. Sauvron, A. M. Mirza, R. Deng, P. J. Mahon, and J. P. Langedijk. 2001. Structural and functional relationship between the receptor recognition and neuraminidase activities of the Newcastle disease virus hemagglutinin-neuraminidase protein: receptor recognition is dependent on neuraminidase activity. J. Virol. 75:1918–1927.

Jiang, W., Y. Cheng, N. Zhao, L. Li, Y. Shi, A. Zong, and F. Wang. 2018. Sulfated polysaccharide of Sepiella Maindroni ink inhibits the migration, invasion and matrix metalloproteinase-2 expression through suppressing EGFR-mediated p38/MAPK and PI3K/Akt/mTOR signaling pathways in SKOV-3 cells. Int. J. Biol. Macromol. 107:349–362.

Jin, J., J. Zhao, Y. Ren, Q. Zhong, and G. Zhang. 2016. Contribution of HN protein length diversity to Newcastle disease virus virulence, replication and biological activities. Sci. Rep. 6:36890.

Kapczynski, D. R., C. L. Afonso, and P. J. Miller. 2013. Immune responses of poultry to Newcastle disease virus. Dev. Comp. Immunol. 41:447–453.

Lu, Y., X. Xu, T. Jiang, L. Jin, X. D. Zhao, J. H. Cheng, X. J. Jin, J. Ma, H. N. Piao, and L. X. Piao. 2019. Sertraline ameliorates inflammation in CUMS mice and inhibits TNF-α-induced inflammation in microglia cells. Int. Immunopharmacol. 67:119–128.

Maan, S., S. K. Mor, N. Jindal, V. G. Joshi, C. Ravishankar, V. K. Singh, R. Ravindran, N. Sahoo, J. Radzio-Basu, M. A. Schilling, W. R. Jr McVey, N. K. Mahajan, V. Kapur, and S. M. Goyal. 2019. Complete genome sequences of Newcastle disease virus isolates from backyard chickens in northern India. Microbiol. Resour. Announc. 8:e00467–e00519.

Mahon, P. J., A. M. Mirza, and R. M. Iorio. 2011. Role of the two sialic acid binding sites on the newcastle disease virus HN protein in triggering the interaction with the F protein required for the promotion of fusion. J. Virol. 85:12079–12082.

Melanson, V. R., and R. M. Iorio. 2006. Addition of N-glycans in the stalk of the Newcastle disease virus HN protein blocks its interaction with the F protein and prevents fusion. J. Virol. 80:623–633.

Nath, B., N. N. Barman, and S. Kumar. 2016. Molecular characterization of Newcastle disease virus strains isolated from different outbreaks in Northeast India during 2014−15. Microb. Pathog. 91:85–91.

Pujol, A. C., J. M. Carlucci, C. M. Matulewicz, and B. E. Damonte. 2007. Natural sulfated polysaccharides for the prevention and control of viral infections. Top Heterocycl. Chem. 11:259–281.

Porotto, M., I. Devito Porotto, S. G. Palmer, E. M. Jurgens, J. L. Yee, C. C. Yokoyama, A. Pessi, and A. Moscona. 2011. Spring-loaded model revisited: paramyxovirus fusion requires engagement of a receptor binding protein beyond initial triggering of the fusion protein. J. Virol. 85:12867–12880.

Porotto, M., Z. Salah, I. DeVito, A. Talekar, S. G. Palmer, R. Xu, I. A. Wilson, and A. Moscona. 2012. The second receptor binding site of the globular head of the Newcastle disease virus hemagglutinin-neuraminidase activates the stalk of multiple paramyxovirus receptor binding proteins to trigger fusion. J. Virol. 86:5730–5741.

Römer-Oberdörfer, A., E. Mundt, T. Mebatsion, U. J. Buchholz, and T. C. Mettenleiter. 1999. Generation of recombinant lentogenic Newcastle disease virus from cDNA. J. Gen. Virol 80:2987–2995.

Shahar, E., R. Haddas, D. Goldenberg, A. Lublin, I. Bloch, N. Bachner Hinenzon, and J. Pitcovski. 2018. Newcastle disease virus: is an updated attenuated vaccine needed? Avian Pathol 47:467–478.

Song, X., Z. Yin, L. Li, A. Cheng, R. Jia, J. Xu, Y. Wang, X. Yao, C. Lv, and X. Zhao. 2013a. Antiviral activity of sulfated Chuanminshen violaceum polysaccharide against duck enteritis virus in vitro. Antivir. Res. 98:344–351.

Song, X., Z. Yin, X. Zhao, A. Cheng, R. Jia, G. Yuan, J. Xu, Q. Fan, S. Dai, H. Lu, C. Lv, X. Liang, C. He, G. Su, L. Zhao, G. Ye, and F. Shi. 2013b. Antiviral activity of sulfated Chuanmingshen violaceum polysaccharide against Newcastle disease virus. J. Gen. Virol. 94:2164–2174.

Song, X., Y. Zhang, Z. Yin, X. Zhao, X. Liang, C. He, L. Yin, C. Lv, L. Zhao, G. Ye, F. Shi, G. Shu, and R. Jia. 2015. Antiviral effect of sulfated Chuanmingshen violaceum polysaccharide in chickens infected with virulent Newcastle disease virus. Virology 476:316–322.

Tanaka, T., Y. Fujishima, S. Hanano, and Y. Kaneo. 2004. Intracellular disposition of polysaccharides in rat liver parenchymal and non-parenchymal cells. Int. J. Pharm. 286:9–17.

Thompson, H. Singh, and D. G. Dalgleish. 2010. Use of surface plasmon resonance (SPR) to study the dissociation and polysaccharide binding of casein micelles and caseins. J. Agric. Food Chem. 58:11962–11968.

Vachali, P., B. Li, K. Nelson, and P. S. Bernstein. 2012. Bernstein. Surface plasmon resonance (SPR) studies on the interactions of carotenoids and their binding proteins. Arch. Biochem. Biophys. 519:32–37.

Wang, Z., C. Jin, X. Li, and K. Ding. 2019. Sulfated polysaccharide JCS1S2 inhibits angiogenesis via targeting VEGFR2/VEGF and blocking VEGFR2/Erk/VEGF signaling. Carbohydr. Polym 207:502–509.

Wang, Z., J. Xie, M. Shen, S. Nie, and M. Xie. 2018. Sulfated modification of polysaccharides: synthesis, characterization and bioactivities. Trends Food Sci. Tech. 74:147–157.

Watrelot, A. A., D. T. Tran, T. Buffeteau, D. Deffieux, C. Le Bourvellec, S. Quideau, and C. M. Renard. 2016. Applied surface science immobilization of flavan-3-ols onto sensor chips to study their interactions with proteins and pectins by SPR. Appl. Surf. Sci. 371:512–518.

Wijesekara, I., R. Pangestuti, and S. K. Kim. 2011. Biological activities and potential health benefits of sulfated polysaccharides derived from marine algae. Carbohydr. Polym. 84:14–21.

Yuan, P., R. G. Paterson, G. P. Leser, R. A. Lamb, and T. S. Jardetzky. 2012. Structure of the ulster strain newcastle disease virus hemagglutinin-neuraminidase reveals auto-inhibitory interactions associated with low virulence. PLoS Pathog. 8 e1002855.

Yuan, P., K. A. Swanson, G. P. Leser, R. G. Paterson, R. A. Lamb, and T. S. Jardetzky. 2011. Structure of the Newcastle disease virus hemagglutinin-neuraminidase (HN) ectodomain reveals a four-helix bundle stalk. Proc. Natl. Acad. Sci. U. S. A 108:14920–14925.

Zhao, J., F. Zhang, X. Liu, K. St Ange, A. Zhang, Q. Li, and R. J. Linhardt. 2017. Isolation of a lectin binding rhamnogalacturonan-I containing pectic polysaccharide from pumpkin. Carbohydr. Polym. 163:330–336.

Zaitsev, V., M. von Itzstein, D. Groves, M. Kiefel, T. Takimoto, A. Portner, and G. Taylor. 2004. Second sialic acid binding site in Newcastle disease virus hemagglutinin-neuraminidase: implications for fusion. J. Virol. 78:3733–3741.